Results in Physics 12 (2019) 1814–1820

Contents lists available at ScienceDirect

Results in Physics

journal homepage: www.elsevier.com/locate/rinp

Investigation of non linear dynamics of an excitable magnetron sputtering plasma

Gopikishan Sabavath[a], Pankaj Kumar Shaw[b], A.N. Sekar Iyengar[c], I. Banerjee[d], S.K. Mahapatra[e,*]

[a] Centre of Plasma Physics – Institute for Plasma Research (CPP-IPR), Sonapur, Assam 782402, India
[b] The Jacob Blaustein Institutes for Desert Research, Ben-Gurion University of the Negev, Midreshet Ben-Gurion, Israel
[c] Plasma Physics Division, Saha Institute of Nuclear Physics, 1/AF, Bidhannagar, Kolkata 700064, India
[d] School of Nano Sciences, Central University of Gujarat, Gandhinagar 382030, India
[e] Centre for Physical Sciences, Central University of Punjab, Bathinda 151001, India

ARTICLE INFO

Keywords:
Intrinsic coherence resonance
Floating potential fluctuation
DC magnetron plasma
Hurst exponent
Noise component

ABSTRACT

In this paper nonlinear dynamical behaviour of an excitable DC magnetron sputtering plasma has been investigated. Initially, plasma exhibited fixed point dynamics whereas with the increase in the discharge voltage, spikes were observed in the floating potential fluctuations. Furthermore, the increasing of discharge voltage resulted the increase in spikes. Power spectrum plot, normalized variance, recurrence plot and Hurst exponent are employed to extract the underlying feature of the floating potential fluctuations. A dip in the plot of normalized variance with variation in the control parameter has been seen, which is strongly indicative of coherence resonance like behaviour in the system. Power spectrum plot and Hurst exponent estimation are confirming the presence of coherence resonance behaviour. Apart from quantitative confirmation, visual verification of coherence resonance behavior has been carried out using recurrence plot analysis. It is noticed that the noise component increases with the increase in the discharge voltage and a suitable intrinsic noise strength plays an important role in generating the coherence resonance.

Introduction

The response of non linear systems to noise has gathered great attention recently. There are several examples signifying that the proper amount of noise can resonantly amplify weak signals which is known as stochastic resonance (SR). The initial contributions in this area are brought by Benzi et al. [1,2] and Nicolis et al. [3], as a possible explanation for climate change on long-time scales. A related phenomenon is coherence resonance (CR), where, even in the absence of a subthreshold deterministic signal, enhanced regularity of the provoked dynamics is observed for optimum strength of superimposed external noise [4–6]. Both SR and CR have been found experimentally and theoretically in various biological [7–11], chemical [12–17], and physical [18–20] non-linear dynamical systems. In comparison to external noise, the role of internal noise and its interaction with system dynamics is less understood. It is possible that the internal noise can play a constructive role in nonlinear systems. Experimentally, it has been shown that synaptic noise improves the detection of subthreshold signals in Hippocampal CA1 neurons [21]. It has also been shown numerically by Schmid et al. [22] using the Hodgkin-Huxley model [23], that internal noise caused by the fluctuations of individual channels in an assembly of ion channels can induce intrinsic coherence resonance (ICR).

ICR is less studied phenomena compared to CR. In ICR phenomena, improved regularity of the inherent system dynamics is provoked by internal noise [24–26]. The existence of ICR was observed only in few experimental systems as experimental control on the internal noise is difficult. ICR was observed during electro dissolution passivation of iron in contact with chloride-containing sulfuric acid solutions ($H_2SO_4 + Na_2SO_4$), where it was demonstrated the internal-noise-provoked resonance phenomena. ICR phenomena was seen by concentration of chloride ions [27]. Inherent noise present ceaselessly in physical collision reaction of the plasma [28,29], plays valuable role in numerous natural systems yielding remarkable results. Various mechanisms like ions collision, electrons collision, secondary electrons or ion emission play important role in generation of intrinsic noise in plasma [30–33]. Since the collision of plasma particles occur quite randomly, it causes the net electric charge fluctuation in time even with the plasma parameters like temperature and number densities are fixed [34]. In this communication, the influence of intrinsic noise to floating potential

* Corresponding author.
E-mail address: sk.mahapatra@cup.edu.in (S.K. Mahapatra).

https://doi.org/10.1016/j.rinp.2019.02.016
Received 31 December 2018; Received in revised form 2 February 2019; Accepted 2 February 2019
Available online 07 February 2019

fluctuations (FPF) has been explored in direct current magnetron sputtering plasma(DCMSP). DCMSP is often characterized by instabilities, revolving spatial structures and anomalous transport. Kudrna et al. demonstrated that the requirement of a certain threshold discharge voltage and pressure to produce fluctuation mode in magnetron sputtering plasma [35]. Martines et al. also confirmed that necessity of threshold neutral pressure and power to create mode in plasma and it was found that with increasing neutral pressure the fluctuations become turbulent [36]. Moreover, theoretically studied $E \times B$ mode and rotating structure in low temperature plasma, give insight to magnetic mode instabilities [37].

In our previous work, Sabavath et al. [38], operating parameters for the experiment were different than present experiment and order to chaos phenomena was found. Under different operating conditions, magnetron sputtering exhibits different behaviour. However, to use this device efficiently one has to operate the device in regular dynamical and maximum power output condition. In the case of intrinsic coherence resonance output of the system is maximum which may be suitable for uniform thin film deposition. Intrinsic noise coherence resonance phenomena is observed in glow discharge plasma by Shaw et al. [39], they have clearly shown that the possibility of finding regular dynamics in the absence of external noise source. Non linear dynamics is widely studied in glow discharge plasma [40,41] than magnetron sputtering plasma. Hence, we have investigated intrinsic noise induced coherence resonance phenomena in magnetron sputtering device. So that one can characterize such device for regular dynamics. In comparison of both the systems, glow discharge plasma system has only E field whereas the magnetron sputtering plasma has both E and B field together. Coherence resonance is a very important dynamical phenomenon in the plasma and it is still a good topic for research. Recently, Fukuyama et al. found coherence resonance phenomena in the coupled plasma oscillator [42]. Other than plasma physics, evidence of intrinsic noise induced coherence resonance phenomena is found in electro chemical oscillator system [43].

In the present work, excitable dynamics of magnetron sputtering plasma has been studied. The possibility of observing regular dynamics in nonlinear systems without adding noise from the outside in a direct current magnetron sputtering plasma is explored. It has been assumed that the observation of ICR in the DC magnetron sputtering plasma will lead to a better understanding of the magnetised plasma dynamics. In order to identify the presence of coherence phenomena in sputtering plasma, power spectrum and newly advanced visual recurrence plot (RP) analysis techniques are used. Statistical observations are carried out using Hurst exponent and normalized variance. Wiener filter and log–log plots of the power spectrum are used to find out the noise component of the signal.

Experimental details

The experiment is carried out in DC magnetron sputtering plasma. The schematic diagram of a DC magnetron sputtering system is shown in Fig. 1. It consists of (a) DC power supply, (b) digital storage oscilloscope (DSO), (c) Wilson-seal port, (d) top flange, (e) cylindrical shaped stainless steel chamber, (f) magnetron sputter gun, (g) target, (h) mass flow controller (MFC) gas flow meter, (i) Langmuir probe (LP), (j) vacuum pump, (k) substrate holder, and (l) bottom flange. Top flange contains sputter magnetron and Langmuir probe setup whereas, bottom flange contains only sample holder.

Plasma is generated in a cylindrical chamber having length and inner diameter of 295 mm and 295 mm respectively. The cathode is connected to high voltage terminal whereas chamber is grounded. 1 kW high voltage power supply is used for discharge. The gas pressure inside the chamber is controlled by MFC and measured using penning and pirani gauges [44].

The chamber is evacuated using a rotary pump followed by a diffusion pump up to a base pressure of 6×10^{-6} mbar and the experiment

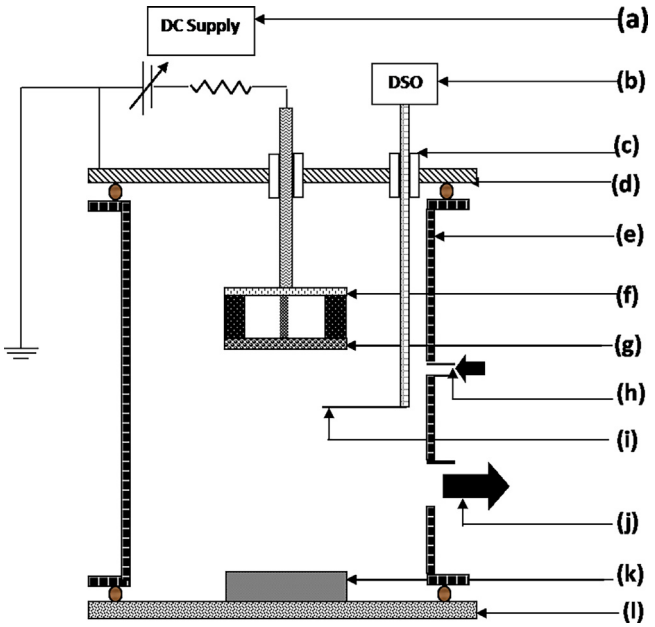

Fig. 1. Schematic diagram of the direct current magnetron sputtering system.

is performed at 4.5×10^{-2} mbar pressure. *TiNi* of 2 inch diameter and 5 mm thickness is used as sputtered target have wide applications [45,46]and argon (*Ar*) is used as sputtering gas. Diameter 0.5 mm and length 10 mm of the cylindrical LP is connected to Agilent DSO for time series spectrum recording. LP is located at 6 cm away from the target and floating potential fluctuations have been recorded using DSO with data length of 10242. The sample time and total time length of the data were 0.2 μs and ~2 ms respectively. Sampling frequency of the data were 5 ms/s. The experiment is performed at a constant working pressure and different discharge voltages. The typical plasma parameters: electron density, electron temperature, and deposition rate were 1×10^{15}–3×10^{15} m^{-3}, 1–3.5 eV and $0.2 - 0.8$ A^0/s, respectively.

The system is a DC magnetron sputtering unit, consists a magnetron (Fig. 2) for the confinement of the plasma and system can be used in thin film deposition. All magnets of the magnetron have the identical strength. The centre one is south pole surrounded by the north poles. The kinetic energy of the movement of electrons with a single path is cycloid. The magnetic crossed electric fields ($E \times B$ drift region) causes confinement of the plasma in front of the cathode which improves the ionization rate. This leads sputtering around a spherical area on the target known as race track. Magnetic measurement of the magnetron and magnetic lines of force are reported in our earlier work [47].

Fig. 2. Magnetron.

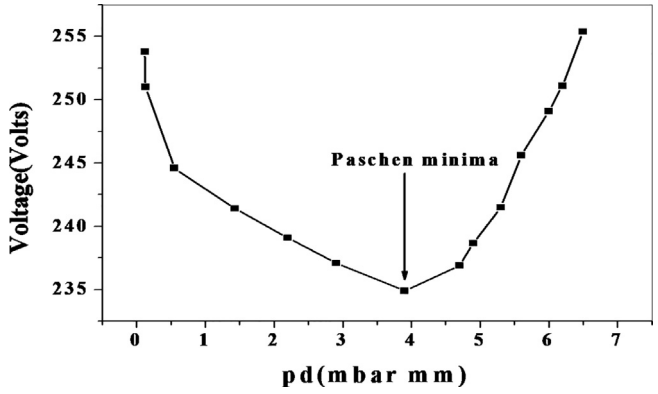

Fig. 3. Paschen curve of the system.

Results and discussions

The Paschen curve (discharge volrage vs. pressure × distance (pd)) of *Ar* in the DC magnetron sputtering system is shown in Fig. 3. The base pressure of the plasma chamber was maintained at 6×10^{-6} mbar. Working pressure is varied by adjusting the *Ar* gas flow rate to the plasma chamber. Initially, at a working pressure (P), the DC voltage was increased slowly to observe the breakdown voltage at constant anode-cathode gap (d = 10 cm). It is observed from the Paschen curve that initially discharge voltage decreases with increase in pd and then increase with pd after going through a minimum value. When it attains a minimum value of breakdown voltage, called Paschen minima, which divide the pressure range in high voltage-low current (LHS of Paschen minimum) and low voltage-high current regime (RHS of the Paschen minimum). Since all the experiments for deposition of thin films in this system is carried out in the region of low voltage and high current regime, present study is carried out in the same region.

Floating potential fluctuations (FPFs) at different discharge voltage (DV) in the range of 392 V to 410 V, obtained in a DC magnetron sputtering plasma, are shown in Fig. 4. It is observed that at 392 V, plasma shows a few excitable spikes, further with increasing DV number of spikes are increased. In Fig. 4(a–e), the separation between the any two consecutive peaks are irregular. At DV of 401 V [Fig. 4(f)], spikes become regular i.e., separation between any two consecutive spikes are regular. With further increasing the DV, system gets back to more irregular oscillations as depicted in the Fig. 4(g–j). Therefore, from Fig. 4 it is observed that at 401 V FPF exhibits comparatively regular dynamics. The approximate values of rise and fall time of the spikes are 6.6–8.2 and 5–5.6 μs respectively. These time scales are comparable with the ion transit time scale($\tau = \frac{d}{\sqrt{\frac{k_b T_i}{m}}} \sim$ few μs, where d, k_b, m and T_i are the electrode distance, Boltzmann constant, ion mass and ion temperature respectively) between two electrodes. So, possibly these spikes correspond to those bunch of ions that are excited from the cathode.

Peak positions on x-axis of FPF plots at different DV is shown in Fig. 5. Peaks positions are denoted by blue points and few irregular peaks are pointed out with ellipse in red colour. Fig. 5 shows number of peaks increased with the increment of DV. In addition to this, regular peaks are observed at 401 V in comparison with its lower DV ranging from 392 V to 400 V and higher DV ranging from 404 V to 410 V. It is considered that oscillations at ~401 V are bounded like coherence resonance.

In order to explore the quantitative measurement of regulatory, normalized variance (NV) has been used. It is defined as *NV = std(tp)/mean(tp)*, where, *tp* is the time interval between two consecutive peaks, *std* is standard deviation. The oscillation having regular occurrence of peaks should have a very small value of NV (0 for exactly periodic occurrence of peaks) and for irregular occurrence of peaks NV will be greater [48]. Fig. 6 shows the variation of NV with discharge voltage (DV). The NV plot is a U-shape curve, where the minimum NV corresponds to the maximal coherence induced at 401 V. Thus oscillations achieved highest regularity at 401 V. Initial dip from 0.85 to 0.42 and final rise from 0.42 to 0.89, suggest that system attained most regular behaviour at the value of 401 V. It is also evident from Fig. 6, that a deeper minimum in the NV curve is observed for more regular spikes. U-Shaped curve of NV is generally observed in the coherence resonance phenomena. As external noise has not been introduced in the present experiment, the above results can be a signature of intrinsic noise induced coherence resonance.

For consolidating the results, the coherence resonance phenomena of the oscillations has been also quantified through estimation of Hurst exponent (H) using R/S statistics [49]. The value of $H = 0.5$, < 0.5, > 0.5, and 1 indicates the random, anticorrelated, correlated, and periodic nature of the time series signal respectively [50]. Hurst exponent vs discharge voltage is presented in Fig. 6. Hurst exponent seems to follow reverse characteristics in comparison to NV with DV. The minimum of NV at 401 V corresponds to maximum of Hurst exponent (0.87). The maximum temporal correlation at 401 V suggests that oscillations are at coherence resonance.

As intrinsic noise is playing a role in the above observation, the intrinsic noise level is estimated. There is no specific way available to measure the intrinsic noise of an experimental system. It is known that experimental signals are contaminated with noise. Thus, by estimating the level of this noisy component of the time series one can get an idea about the intrinsic noise. Here, Wiener filter [51] subroutine of matlab has been used to estimate the noise strength which is shown in the Fig. 7. It is observed that intrinsic noise level is increased with increment of DV. Variation in DV causes nonlinear oscillations, excitable dynamics in plasma and enhancement of the intrinsic noise level. Hence, change in DV can lead to two effects: 1) change in the plasma characteristics 2) change in the internal noise of the system [52]. Present experiment is performed in very small windows of DV (410 V–392 V = 18 V). This small range of DV is not enough to change the plasma characteristic significantly. So, the second effect will be more significant in the case of excitable system. Thus, maximum regularity is achieved at optimum value of noise strength and the observed phenomena can be called intrinsic noise induces coherence resonance.

Power spectrum is one of the methods which can be used to prove the maximum power concentred in the narrow band at coherence resonance. In the present case, response of power spectrum is expected to become maximal when ICR occurs at a certain applied potential value. Fig. 8 shows the power spectrum plots at a) 392 V, b) 401 V and c) 408 V. The system exhibits the sharp peak in resonance window [Fig. 8(b)] than the off resonance windows [Fig. 8(a) and Fig. 8(c)]. Resonance window shows the highest power than other power spectrum plots at respective applied discharge voltage. Upon increasing the discharge voltage, the system reaches a maximum power at 401 V, indicating the occurrence of ICR. Similar power spectrum plots are observed for experimental evidence of coherence resonance in an optical system, i.e., regularity of the excitable pulses in the intensity of a laser diode with increasing optical feedback by adding noise, up to an optimal value of the noise strength [53]. This type of induced coherence is useful to streamline the deposition mechanism for sputtering system thereby exciting the oscillation. Since regular dynamics are related to ion transit mode which is enhanced by intrinsic noise at particular level, this phenomena can be considered as intrinsic noise induced coherence resonance.

Change in the noise level with discharge voltage has been confirmed by estimating noise strength using the log – log plot of power spectrum. A typical log log spectra at 392 V is shown in Fig. 9. Depending on the value of log(power), this plot has been separated in two frequency regions. Noisy and actual signal regions are assigned in Fig. 9. Noisy data has been elected by a straight line as shown in figure and sum of the power of respective data points from original power spectrum plot

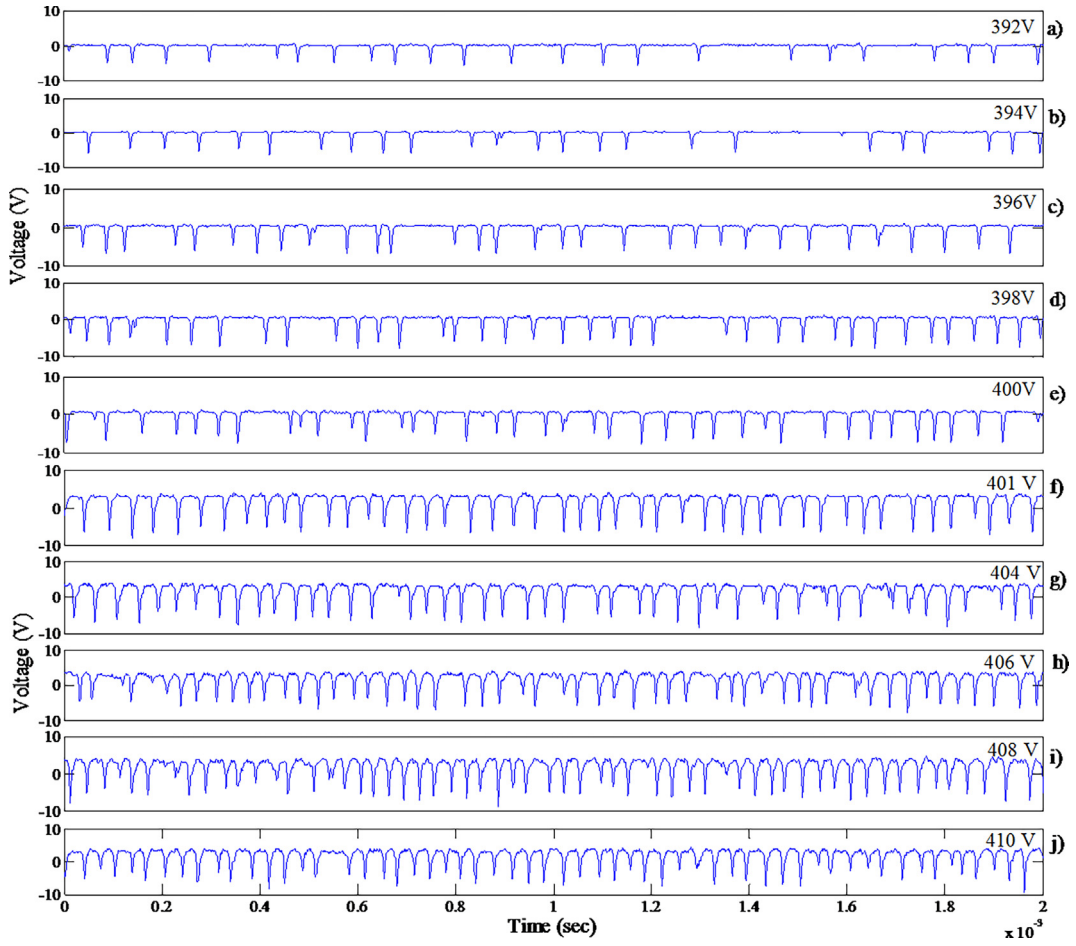

Fig. 4. Floating potential fluctuations at different discharge voltages: (a) 392 V, (b) 394 V, (c) 396 V, (d) 398 V, (e) 400 V, (f) 401 V, (g) 404 V, (h) 406 V, (i) 408 V, (j) 410 V.

provides the noise level, i.e., $g = (x_{(i)} + x_{(i+1)} + x_{(i+2)} + --------+x_{(i+n)})$, where i is the initial point of frequency corresponds to noise signal and x is corresponding power in power spectra. It is observed that noise level gradually increases with increase in the discharge voltage as shown in Fig. 10, which is well supported by Weiner filter.

Recurrence plot (RP) is frequently used advanced technique introduced in late 1980s by Ekmann to visualize the recurrences of dynamical systems [54]. RP can find the hidden periodicity in a time series signal which is developed based on reconstructed phase space. Experimental observation produces a sequence of scalar measurements which is presented by a given time series x_i (i = 1, 2, 3,……,N) and it is

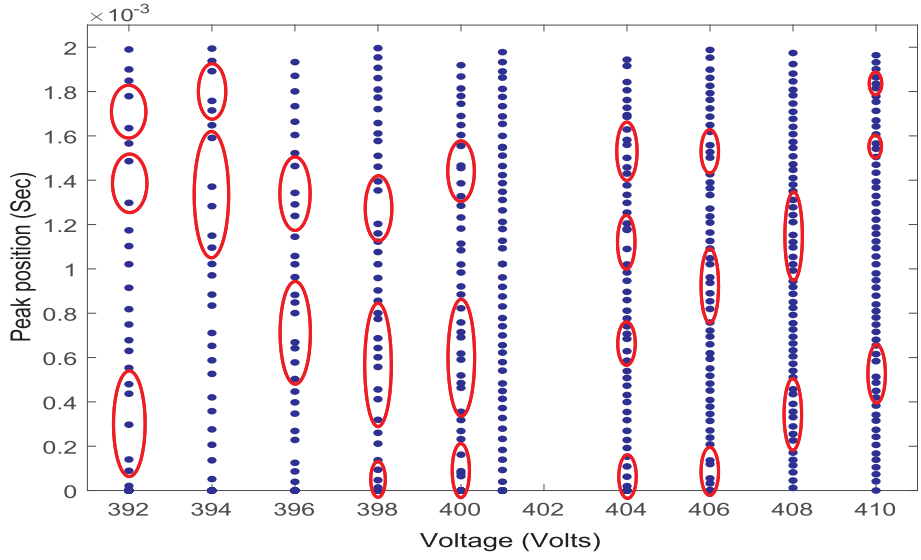

Fig. 5. Peaks position from FPF plots as a function of discharge voltage. Separation between two points depicts distance among the peaks.

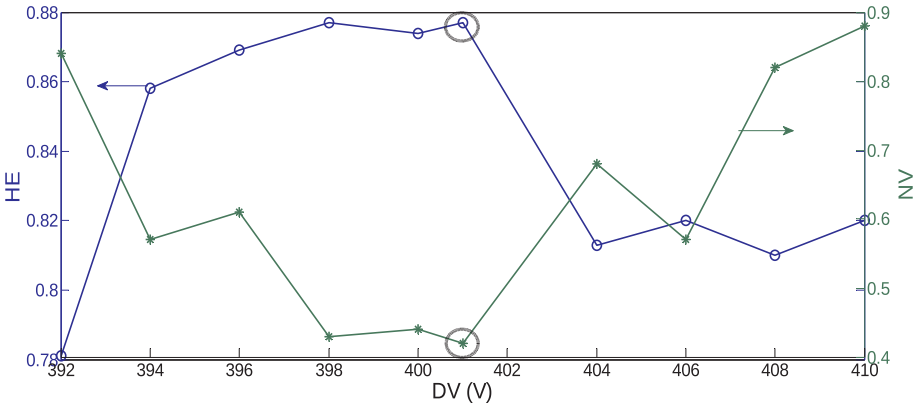

Fig. 6. Plot of normalized variance (NV) (right-hand side y-axis) and the Hurst exponent (HE) (left-hand side y-axis) against the DV.

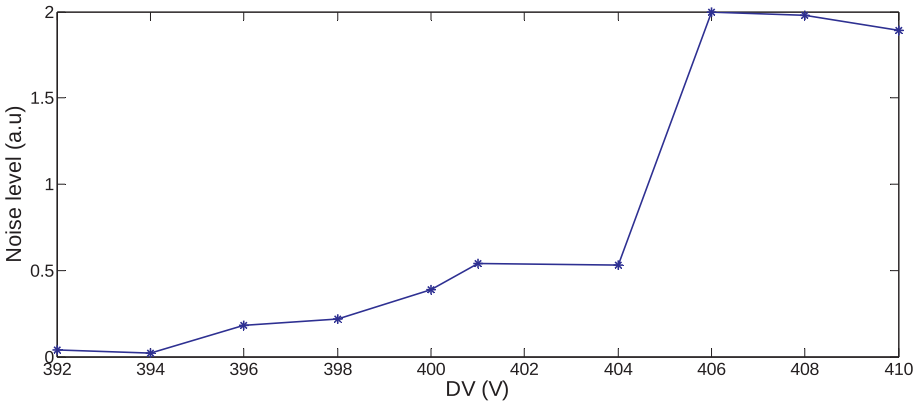

Fig. 7. Intrinsic noise level from Weiner filter subroutine of Matlab.

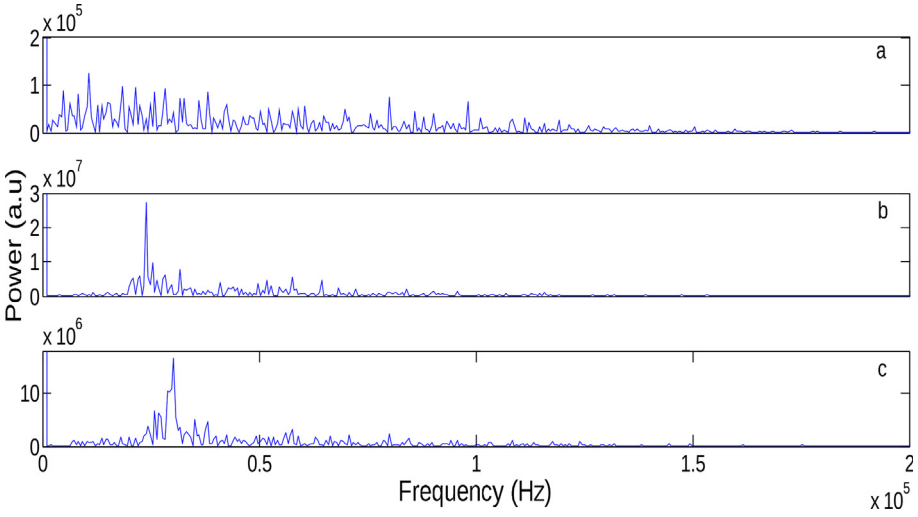

Fig. 8. Power spectra for the floating potential fluctuations at DV a) 392 V, b) 401 V and c) 408 V.

reconstructed to high dimensional phase space by providing embedding dimension and time delay using false nearest neighbour and auto correlation respectively. The RP is expressed as a two dimensional square matrix. RP represents the occurrence with ones and zeroes for states of $\vec{x_i}$ and $\vec{x_j}$ of the system.

$$R_{i,j} = H(\varepsilon - ||\vec{x_i} - \vec{x_j}||), (i, j = 1, 2, ...,M) \quad (1)$$

where M is the number of data points of the signal, H is the heaviside function and ||. || is the norm (Euclidean norm). ε is the choice of the threshold. We have chosen approximately 0.5% point density. The matrix evaluates the states of the system at times i and j. Similar states represented in the matrix by one, i.e. $R_{i,j} = 1$ and structure the uniformity in recurrence along the diagonal line. On the other side if states are dissimilar, the resultant entry in the matrix is $R_{i,j} = 0$ and produces non uniformity of diagonal structure of the RP. From all the above properties, recurrence plot can be used as a better visual confirmation technique for coherence resonance. Because some time it is very difficult to understand the coherence resonance phenomena just by looking at the time series data. Fig. 11 shows the recurrence plots at three different discharge voltages a) 392 V, b) 401 V and c) 408 V. In Fig. 11b, much regular diagonal lines is seen whereas no regular pattern is seen

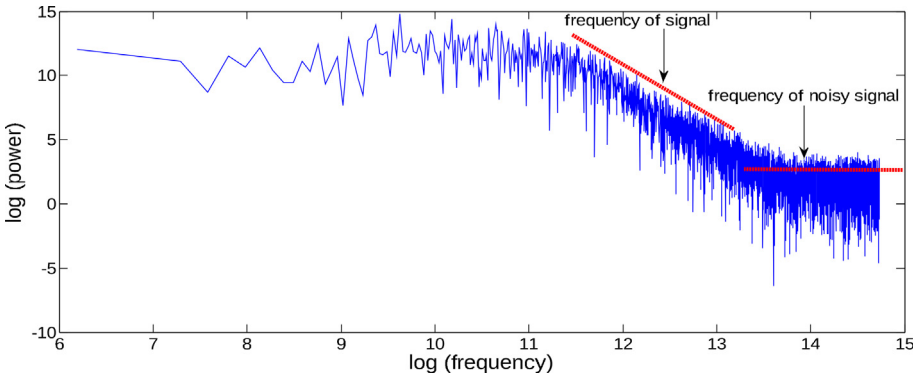

Fig. 9. Log-log plot of the power spectrum at signal 392 V.

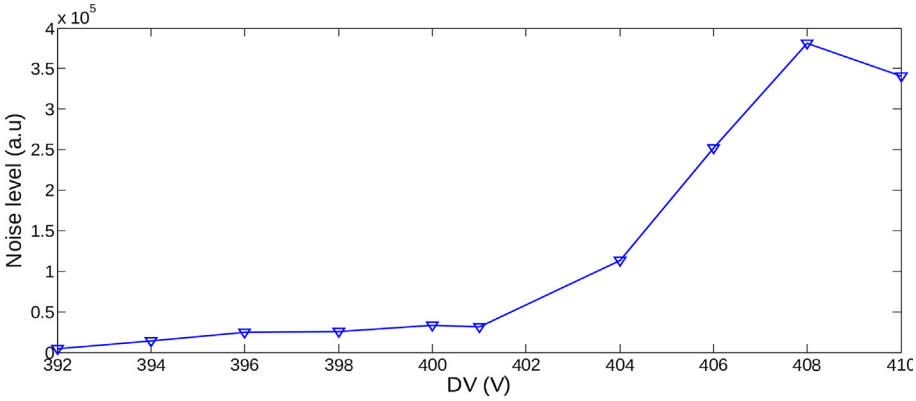

Fig. 10. Intrinsic noise level from log – log plots.

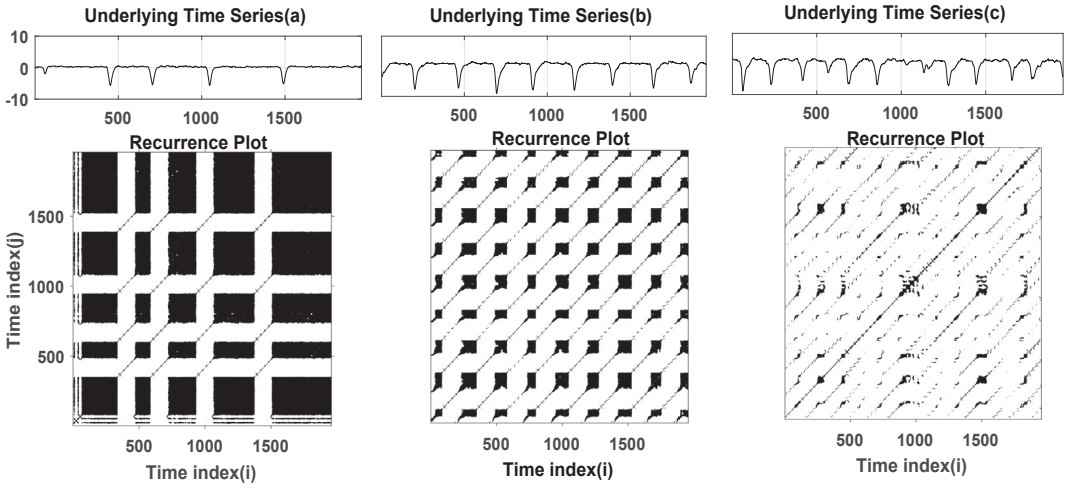

Fig. 11. Recurrence plot for the floating potential fluctuations at DV a) 392 V, b) 401 V and c) 408 V.

in the other two plots (Fig. 11a and Fig. 11c). Here, the visual representation is very transparent to look at the regular dynamics as compare to the other tools. It is also confirming that at 401 V of discharge voltage system is governing the coherence phenomenon.

Conclusion

The effect of the intrinsic noise of an excitable plasma system has been observed in the form of intrinsic noise induced coherence resonance. It is noticed that intrinsic noise component is increased with the increasing discharge voltage. System attained most regular behavior at optimum value of intrinsic noise and plays an important role in the generation of the coherence resonance. Normalized variance curve is used to quantify the regularity of spiky oscillation. Power spectrum plots also confirmed the presence of coherence resonance phenomena. Here, it is established that recurrence plot ia a very useful tool to visualize and identification of coherence resonance phenomena. In our experiment, magnetic field is constant and the corresponding frequency of $E \times B$ mode is approximately 20–50 kHz which has been appeared in the broadband range of measured frequencies. Optimum regularity in floating potential fluctuation and maximum power in power spectrum is exhibited at the point of coherence resonance. Coherence in magnetron sputtering plasma can be controlled by choosing a proper intrinsic noise region. Plasma fluctuation investigation is important from a practical point of view since magnetron sputtering devices are used to develop thin flim/nanoparticle growth and there are few reported

works which indicate the correlation between plasma fluctuation and fluctuations of nanoparticle growth [55]. The investigation on correlation between plasma fluctuation and growth of nano particles under various dynamical conditions to obtain the uniform thin films will be our future work.

Acknowledgement

The authors would like to thank, SINP director, Ajit Kumar Mohanty for local hospitality in their guest house and Debajyoti Saha for some fruitful discussion.

Appendix A. Supplementary data

Supplementary data associated with this article can be found, in the online version, athttps://doi.org/10.1016/j.rinp.2019.02.016.

References

[1] Benzi R, Sutera A, Vulpiani A. The mechanism of stochastic resonance. J Phys A 1981;14:L453–7.
[2] Benzi R, Parisi R, Sutera A, Vulpiani A. Stochastic resonance in climatic change. Tellus 1982;34:10–6.
[3] Nicolis C. Stochastic aspects of climatic transitions – response to a periodic forcing. Tellus 1982;34:1–9.
[4] Pikovsky AS, Kurths J. Coherence resonance in a noise-driven excitable system. Phys Rev Lett 1997;78:775–8.
[5] Giacomelli DG, Giudici M, Balle S, Tredicce JR. Experimental evidence of coherence resonance in an optical system. Phys Rev Lett 2000;84:3298–301.
[6] Neiman A, Saparin PI, Stone L. Coherence resonance at noisy precursors of bifurcations in nonlinear dynamical systems. Phys Rev E 1997;56:270–3.
[7] Lee CY, Choi W, Han JH, Strano MS. Coherence resonance in a single-walled carbon nanotube ion channel. Science 2010;329:1320–4.
[8] Russell DF, Wilkens LA, Moss F. Use of behavioural stochastic resonance by paddle fish for feeding. Nature 1999;402:291–4.
[9] Simonotto E, Riani M, Seife C, Roberts M, Twitty J, Moss F. Visual perception of stochastic resonance. Phys Rev Lett 1997;78:1186–9.
[10] Lee SG, Neiman A, Kim S. Coherence resonance in a Hodgkin-Huxley neuron. Phys Rev E 1998;57:3292–7.
[11] Zhou CS, Kurths J, Hu B. Array-enhanced coherence resonance: nontrivial effects of heterogeneity and spatial independence of noise. Phys Rev Lett 1997;87:09810.
[12] Beato V, Sendina-Nadal I, Gerdes I, Engel H. Coherence resonance in a chemical excitable system driven by coloured noise. Philos Trans R Soc A 2008;366:381–95.
[13] Miyakawa K, Isikawa H. Experimental observation of coherence resonance in an excitable chemical reaction system. Phys Rev E 2002;66:046204.
[14] Amemiya T, Ohmori T, Yamamoto T, Yamaguchi T. Stochastic resonance under two-parameter modulation in a chemical model system. J Phys Chem A 1999;103:3451–4.
[15] Miyakawa K, Isikawa H. Experimental observation of coherence resonance in an excitable chemical reaction system. Phys Rev E 2002;66:046204.
[16] Escalera SGJ, Rivera M, Parmananda P. Experimental evidence of coexisting periodic stochastic resonance and coherence resonance phenomena. Phys Rev Lett 2004;92:230601.
[17] Escalera SGJ, Rivera M, Escalova J, Parmananda P. Interaction of noise with excitable dynamics. Philos Trans R Soc A 2008;366:369–80.
[18] Dinklage A, Wilke C, Klinger T. Spatio-temporal response of stochastic resonance in an excitable discharge plasma. Phys Plasmas 1999;6:2968–71.
[19] Nurujjaman M, Sekar Iyengar AN, Parmananda P. Emergence of the stochastic resonance in glow discharge plasma. J Phys 2010;208:012084.
[20] Nurujjaman M, Iyengar ANS, Parmananda P. Noise-invoked resonances near a homoclinic bifurcation in the glow discharge plasma. Phys Rev E 2008;78:026406.
[21] Stacey WC, Dominique DM. Noise and coupling affect signal detection and bursting in a simulated physiological neural network. J Neurophysiol 2001;86:1104.
[22] Schmid G, Goychuk I, Hanggi P. Stochastic resonance as a collective property of ion channel assemblies. Europhys Lett 2001;56:22–8.
[23] Hodgkin AL, Huxley AF. A quantitative description of membrane current and its application to conduction and excitation in nerve. J Physiol (London) 1952;117:500–44.
[24] Hou ZH, Xin HW. Internal noise stochastic resonance in a circadian clock system. J Chem Phys 2003;119:11508–12.
[25] Dey S, Das D, Parmananda P. Intrinsic noise induced resonance in presence of subthreshold signal in Brusselator. Chaos 2011;21:033124.
[26] Schmid G, Hanggi P. Intrinsic coherence resonance in excitable membrane patches. Math Biosci 2007;207:235–45.
[27] Escalera SGJ, Rivera M, Escalova J, Parmananda P. Interaction of noise with excitable dynamics. Philos Trans R Soc A 2008;366:369–80.
[28] Shotorban B. Bistable intrinsic charge fluctuations of a dust grain subject to secondary electron emission in plasma. Phys Rev E 2015;92:043101.
[29] Salehi M, Zavarian AA, Arman A, Hafezi F, Rad GA, Mardani M, Hamze K, Luna C, Naderi S, Ahmadpourian A. Characterization of the ion beam current density of the RF ion source with flat and convex extraction systems. Silicon 2018;10:2473–749.
[30] Ivan LM, Dimitriu DG, Niculescu O, Sanduloviciu M. On the complex self-organized systems created in laboratory. J Optoelectron Adv Mater J 2008;10:1950–3.
[31] Dimitriu DG, Ignatescu V, Ionita C, Lonzneanu E, Sanduloviciu M, Schrittwieser RW. The influence of electron impact ionisations on low frequency instabilities in a magnetised plasma. Int J Mass Spectrom 2003;224:141–58.
[32] Mariammal M, Bornali S, Vramori M, Hari Prakash N, Arun S. Oscillating plasma bubble and its associated nonlinear studies in presence of low magnetic field. Phys Plasmas 2016;23(7):072102.
[33] Vramori M, Bornali S, Arun S, Janaki MS, Sekar Iyengar AN, Marwan N, Kurths J. Investigation of complexity dynamics in a DC glow discharge magnetized plasma using recurrence quantification analysis. Phys Plasmas 2016;23(6):062312.
[34] Shotorban B. Bistable intrinsic charge fluctuations of a dust grain subject to secondary electron emission in plasma. Phys Rev E 2015;92:043101.
[35] Kudrna P, Holik M, Bilyk O, Marek A, Behnke JF. Langmuir Probe Study of the Floating Potential Fluctuations in the DC Cylindrical Magnetron Discharge. International Conference on Phenomena in Ionized Gases [26th] Held in Greifswald, Germany 2003; 4.
[36] Martines E, Cavazzana R, Serianni G, Spolaore M, Tramontin L, Zuin M, Antoni V. Electrostatic fluctuations in a direct current magnetron sputtering plasma. Phys Plasmas 2001;8:3042.
[37] Boeuf JP. Rotating structures in low temperature magnetized plasmas-insight from particle simulations. Front Phys 2014;2:1–17.
[38] Gopi Kishan S, Pankaj Kumar S, Sekar Iyengar AN, Banerjee I, Mahapatra SK. Experimental investigation of quasiperiodic-chaotic-quasiperiodic-chaotic transition in a direct current magnetron sputtering plasma. Phys Plasmas 2015;22:082121.
[39] Pankaj Kumar S, Debajyoti S, Sabuj G, Janaki MS, Sekar Iyengar AN. Intrinsic noise induced coherence resonance in a glow discharge plasma. Chaos 2015;25:043101.
[40] Alex P, Saravanan A, Jayaprakash K, Suraj KS. Order-chaos-order-chaos transition and evolution of multiple anodic double layers in glow discharge plasma. Results Phys 2015;5:235–40.
[41] Wilson RB, Podder NK. Observation of period multiplication and instability in a dc glow discharge. Phys Rev E 2017;76:046405.
[42] Fukuyama T, Okugawa M. Dynamic characterization of coupled nonlinear oscillators caused by the instability of ionization waves. Phys Plasmas 2017;24:032302.
[43] Rivera M, Escalera Santos GJ, Uruchurtu-Chavarın J, Parmananda P. Intrinsic coherence resonance in an electrochemical cell. Phys Rev E 2005;72:030102(R).
[44] Zavarian AA, Arman A, Ghotbi SMJ, Korpi AG, Salehi M, Mardani M, Hafezi F, Shafiekhani A, Talu S, Afghan AS. Behaviors of capacitive and Pirani vacuum gauges. Vak Forsch Prax 2018;30:39–44.
[45] Davoud D, Arun B. Solution processable sol-gel derived titania gate dielectric for organic field effect transistors. J Mater Sci: Mater Electron 2016;28:3851–9.
[46] Davoud D, Suresh WG, Nandu BC. Studies on electrical properties of hybrid polymeric gate dielectrics for field effect transistors. Macromol Symp 2015;347:81–6.
[47] Gopikishan S, Banerjee I, Mahapatra SK. RP and RQA analysis for floating potential fluctuations in a DC magnetron sputtering plasma. Fluctuation Noise Lett 2016;15:1650011.
[48] Nurujjaman Md, Sekar Iyengar AN, Parmananda P. Noise-invoked resonances near a homoclinic bifurcation in the glow discharge plasma. Phys Rev E 2008;78:026406.
[49] Nurujjaman M, Sekar Iyengar AN. Realization of SOC behavior in a dc glow discharge plasma. Phys Lett A 2007;360:717–21.
[50] Carbone A, Castelli G, Stanley HE. Time dependent Hurst exponent in financial time series. Physica A 2004;344:267–71.
[51] Meyer J, Simmer KU. Multi-channel speech enhancement in a car environment using Wiener filtering and spectral subtraction. IEEE International Conference 1997;2:1167–70.
[52] Stan C, Cristescu CP, Chiriac S, Dimitriu DG. Noise induced change in the dynamics of anodic double layers. Rom J Phys 2009;54:699–704.
[53] Giacomelli G, Giudici M, Balle S, Tredicce JR. Experimental evidence of coherence resonance in an optical system. Phys Rev Lett 2000;84:3298–301.
[54] Eckmann JP, Kamphorst SO, Ruelle D. Recurrence plots of dynamical systems. Eur Phys Lett 1987;4:973–7.
[55] Shiratani M, Koga K, Kamataki K, Iwashita S, Uchida G, Seo H, Itagaki N. Theory for correlation between plasma fluctuation and fluctuation of nanoparticle growth in reactive plasmas. Jpn J Appl Phys 2014;53:010201.